

ORIGINAL ARTICLE

# Primary Human Hepatocytes Repopulate Livers of Mice After *In Vitro* Culturing and Lentiviral-Mediated Gene Transfer

Jeanette Bierwolf, PhD,<sup>1</sup> Tassilo Volz, PhD,<sup>2</sup> Marc Lütgehetmann, MD,<sup>2,3</sup> Lena Allweiss, PhD,<sup>2</sup> Kristoffer Riecken, PhD,<sup>4</sup> Michael Warlich, PhD,<sup>2</sup> Boris Fehse, PhD,<sup>4</sup> Joerg C. Kalff, MD,<sup>1</sup> Maura Dandri, PhD,<sup>2,5</sup> and Joerg-Matthias Pollok, MD, PhD<sup>1</sup>

Cell-based therapies represent a promising alternative to orthotopic liver transplantation. However, therapeutic effects are limited by low cell engraftment rates. We recently introduced a technique creating human hepatocyte spheroids for potential therapeutic application. The aim of this study was to evaluate whether these spheroids are suitable for engraftment in diseased liver tissues. Intrasplenic spheroid transplantation into immunodeficient uPA/SCID/beige mice was performed. Hepatocyte transduction ability prior to transplantation was tested by lentiviral labeling using red-green-blue (RGB) marking. Eight weeks after transplantation, animals were sacrificed and livers were analyzed by immunohistochemistry and immunofluorescence. To investigate human hepatocyte-specific gene expression profiles in mice, quantitative real-time-PCR was applied. Human albumin and alpha-1-antitrypsin concentrations in mouse serum were quantified to assess the levels of human chimerism. Precultured human hepatocytes reestablished their physiological liver tissue architecture and function upon transplantation in mice. Positive immunohistochemical labeling of the proliferating cell nuclear antigen revealed that human hepatocytes retained their *in vivo* proliferation capacity. Expression profiles of human genes analyzed in chimeric mouse livers resembled levels determined in native human tissue. Extensive vascularization of human cell clusters was detected by demonstration of von Willebrand factor activity. To model gene therapy approaches, lentiviral transduction was performed *ex vivo* and fluorescent microscopic imaging revealed maintenance of RGB marking *in vivo*. Altogether, this is the first report demonstrating that cultured and retroviral transduced human hepatocyte spheroids are able to engraft and maintain their regenerative potential *in vivo*.

## Introduction

**T**HERAPEUTIC APPLICATION of primary human hepatocytes as an alternative to liver transplantation represents a promising model for patients with liver-based metabolic disorders or hepatic failure. Data from small animal models indicate that successful hepatocyte transplantation of 5–10% of liver cell mass is required to correct inherited metabolic diseases.<sup>1</sup> For liver regeneration in patients with fulminant hepatic failure it has been estimated that 1–5% of liver mass will be needed.<sup>2</sup> Furthermore, hepatocyte transplantation has been suggested as bridging therapy until a suitable donor organ becomes available in fulminant liver failure or in patients with

metabolic disorders.<sup>3,4</sup> The excellent regenerative potential of the liver also supports the hope for native liver regeneration after clinical liver cell transplantation.<sup>5</sup>

Nevertheless, intraportal hepatocyte transplantation using freshly isolated cells has not yet been routinely established in clinical practice, but first clinical case reports demonstrated principle feasibility and safety of this technique.<sup>6–9</sup> Relatively small cell numbers could theoretically restore liver function *in vivo*. So far, the success of intraportal hepatocyte transplantation using single-cell suspensions has been limited by the low rates of cell engraftment achieved and marginal beneficial effects obtained,<sup>10</sup> thus indicating that the development of new technologies enabling hepatocyte regeneration before transplantation may be required.

The works were performed at the University Medical Centers Bonn and Hamburg-Eppendorf.

<sup>1</sup>Department for General, Visceral, Thoracic, and Vascular Surgery, University Medical Center Bonn, Bonn, Germany.

Departments of <sup>2</sup>Internal Medicine and <sup>3</sup>Medical Microbiology, Virology and Hygiene, University Medical Center Hamburg-Eppendorf, Hamburg, Germany.

<sup>4</sup>Department of Stem Cell Transplantation, Research Department Cell and Gene Therapy, University Medical Center Hamburg-Eppendorf, Hamburg, Germany.

<sup>5</sup>German Center for Infection Research, Hamburg-Lübeck-Borstel Partner Site, Hamburg, Germany.

© Jeanette Bierwolf, 2016; Published by Mary Ann Liebert, Inc. This Open Access article is distributed under the terms of the Creative Commons Attribution Noncommercial License (<http://creativecommons.org/licenses/by-nc/4.0/>) which permits any noncommercial use, distribution, and reproduction in any medium, provided the original author(s) and the source are credited.

Another problem in cell transplantation includes the lack of storing opportunities for highly differentiated human hepatocytes due to the rapid loss of hepatocyte functions that is commonly observed under the currently used two-dimensional (2D) culture conditions.<sup>11</sup> Moreover, previous studies showed that cryopreserved hepatocytes are frequently not suitable for clinical cell transplantation due to their significantly reduced cell attachment.<sup>12</sup>

Hepatocyte morphology and function have been shown to be better maintained by tissue engineering methods using hepatocyte culture on three-dimensional (3D) scaffolds.<sup>13–19</sup> Alginate is a naturally occurring anionic biopolymer typically obtained from brown seaweed. It has been extensively investigated and used for a broad range of tissue engineering applications due to its biocompatibility, low toxicity, and relatively low cost.<sup>20</sup> Another advantage is that scaffolds based on alginate can be dissolved without any cytotoxicity to enable harvesting of cultured cells. We previously created functional human hepatocyte spheroids by preculturing the cells for 7 days on alginate bioscaffolds.<sup>19</sup> We propose that this technique provide a means to enhance cell engraftment rates in the recipient liver by applying spheroid transplantation after scaffold dissolving as an alternative to single-cell application. Moreover, hepatocyte preculturing may offer opportunities for cell analysis, therapeutic gene manipulation, or simply to bridge the availability of highly differentiated hepatocytes from a donor liver if the recipient is temporary not available. To assess some of these possibilities, we now performed transplantation of precultured spheroids into uPA/SCID/beige (USB) mice. In this mouse model of liver regeneration, overexpression of the uPA transgene leads to liver damage, which turns into a cell growth advantage of xenotransplanted hepatocytes, while the SCID beige mutation ensures the necessary immunological tolerance.<sup>21–23</sup>

In brief, the aim of our experiments was to determine whether *ex vivo* engineered and culture-derived human hepatocyte spheroids are suitable to reconstitute the diseased liver of recipient animals.

## Materials and Methods

Full methods are available in the Supplementary Data section (Supplementary Data are available online at [www.liebertpub.com/tea](http://www.liebertpub.com/tea)).

### Bioscaffolds for 3D cell culture

Alginate bioscaffolds in 24-well plates (AlgiMatrix™ 3D Culture System, Cat. No. 12684–023) were purchased from Invitrogen (Carlsbad, CA). Directly before use, the scaffolds were transferred to a 24-well culture plate (Corning, Lowell, MA).

### Isolation of primary human hepatocytes

The study was approved by the Ethical Review Committee of the Rheinische Friedrich-Wilhelms-Universität Bonn (021/12) and the committee of the Ärztekammer Hamburg (WF-021/11). Handling of the human material was performed in accordance with national guidelines, the 1975 Declaration of Helsinki, and after informed consent in writing from each patient's parents. Primary human hepatocytes were isolated from the liver tissue of five children. The first four children underwent liver transplantation due to metabolic diseases or hepatoblastoma, and hepatocytes from these donors were isolated from the explanted livers. One patient underwent size reduction due to relative liver hypertrophy in the context of omphalocele. Hepatocytes from this donor were isolated from the resected liver tissue. Table 1 displays the donor characteristics in details. Samples of organ tissues were flash frozen and stored at  $-80^{\circ}\text{C}$  before starting the cell isolation procedure. Right after explantation/resection hepatocytes were isolated as described earlier.<sup>19</sup> Samples of cells were flash frozen in liquid nitrogen immediately after the isolation procedure and stored at  $-80^{\circ}\text{C}$  for further analysis.

### Cell seeding and culture conditions

The alginate bioscaffolds were seeded with 200  $\mu\text{L}$  cell suspension per scaffold containing  $1 \times 10^6$  hepatocytes. Cells were cultured in 400  $\mu\text{L}$  supplemented William's Medium E without L-Glutamine (Invitrogen) per well as described previously.<sup>19</sup> Cell culture medium was furthermore supplemented from day 3 onward with 2% DMSO, 2 mM 3-methylcholanthrene, and 10 mM dexamethasone (Sigma Aldrich, St. Louis, MO) for cytochrome P450 (CYP) isoenzyme induction.<sup>11</sup> The scaffolds were incubated in a humidified atmosphere of 5%  $\text{CO}_2$  and 95% air at  $37^{\circ}\text{C}$  during 7 days. Culture medium was changed every 24 h.

### RGB marking and lentiviral transduction

In experiment C hepatocyte transduction ability was tested before transplantation using a principle named red-green-blue (RGB) marking.<sup>24</sup> Lentiviral Gene Ontology (LeGO) vectors each expressing one of the three fluorescent proteins (mCherry = red, Venus = green, Cerulean = blue) were designed as described.<sup>24,25</sup>

Target cells were simultaneously transduced 24 h pre-transplant with a multiplicity of infection (MOI) of 20 for each fluorescent protein achieving an overall MOI of 60 (given MOIs are calculated relatively to the titration cell line HEK-293T).

### Spheroid harvesting and transplantation in USB mice

After 7 days of preculture the bioscaffolds were transferred to a centrifugation tube and dissolved as previously

TABLE 1. DONOR AND ISOLATION CHARACTERISTICS

Patient	Donor age/sex	Donor diagnosis	Time of cold ischemia (hours)	Cell viability (%)
A	18 years/m	Primary Oxalosis	48	95
B	4 months/m	Maple syrup urine disease	16	75
C	2 months/m	Maple syrup urine disease	7	99
D	2 years/m	Hepatoblastoma	21	70
E	14 days/w	Size reduction due to relative liver hypertrophy by omphalocele	18	98
Average viability $\pm$ Standard deviation (%)				87.4 $\pm$ 12.3

described.<sup>19</sup> In experiment C, applying RGB marking, spheroids were analyzed by fluorescence microscopy before transplantation to estimate transduction efficiency.

USB mice were originally generated by crossing *Alb-uPA* mice (strain TgN(Alb1Plau)144Bri; The Jackson Laboratory, Bar Harbor, ME) with homozygous SCID/beige mice (strain C.b-17/GbmsTac-SCID/bgN7; Taconic Farms, New York, NY). USB mice were housed and maintained under specific pathogen-free conditions in accordance with institutional guidelines under approved protocols. The presence of the urokinase-type plasminogen activator (uPA) transgene and maintenance of the severe combined immunodeficiency (SCID/beige) phenotype were determined as reported.<sup>26</sup> All animal experiments were conducted in accordance with the European Communities Council Directive (86/EEC), and were approved by the city of Hamburg, Germany (47/11, 15/12, 66/12).

Three-week-old mice were anesthetized with isoflurane and injected intrasplenically with  $1 \times 10^6$  precultured human hepatocytes forming spheroids. After 8 weeks, animals were sacrificed, livers and spleens were explanted, and snap frozen in liquid nitrogen for RNA isolation. Livers from mice transplanted with RGB-marked human hepatocytes underwent treatment as described earlier.<sup>24</sup>

#### Human albumin and alpha-1-antitrypsin assays

To verify repopulation of mouse livers with human hepatocytes, human albumin and alpha-1-antitrypsin (A1A) concentration in mouse serum was measured 8 weeks after transplantation by enzyme-linked immunosorbent assay (ELISA) using a human albumin or human A1A quantification kit (ICL, Newberg, OR), respectively.

#### Immunohistochemical analysis

To proof the presence of zonation immunohistochemical labeling of arginase 1 (ARG1) and glutamine synthetase (GLUL) was performed applying a periportal or perivenous marker, respectively. Furthermore, immunohistochemical labeling of the proliferating cell nuclear antigen (PCNA) and A1A was performed. To display human hepatocyte clusters in mouse livers cryosections (6  $\mu$ m) were immunohistochemically stained with a mouse monoclonal antibody against human cytokeratin 18 (humCK18). All antibodies used for immunohistochemical stainings are listed in Supplementary Table S1. For visualization the En-Vision G2 double-staining system (Dako) was applied in addition to hematoxylin background staining. All sections were analyzed by light microscopy.

#### Immunofluorescence analysis

Human-specific cytoskeletal marker cytokeratin 18 (humCK18) was stained as described<sup>19</sup> to visualize human clusters in mouse livers and spleens. Furthermore, morphological characteristics and activity of hepatocyte-specific factors in livers were demonstrated as detailed in Supplementary Table S2. For the detection of bile canaliculi the sections were incubated with Alexa 488-labeled Phalloidin (Invitrogen; 1:50, 1 h) to stain actin filaments in green. Hoechst 33258 (Invitrogen) was used as counterstaining for viable cell nuclei (1:20,000, 1 min).

All sections were visualized by fluorescence microscopy.

#### RNA isolation and reverse transcription PCR

RNA isolation and reverse transcription were performed in three of the five experiments (patient A, B, and C). After harvesting at day 1 and 7 of cell culture the scaffolds were dissolved. The released cells/spheroids were incorporated into 350  $\mu$ L RLT-buffer (Qiagen, Hamburg, Germany) and 3.5  $\mu$ L  $\beta$ -mercaptoethanol (Sigma-Aldrich). The same process was performed with the native human tissue before cell isolation, the cells frozen directly after isolation and the humanized mouse livers after explantation. The total RNA was extracted from the lysate using RNeasy Mini Kit (Qiagen). For cDNA synthesis the First Strand cDNA Synthesis Kit for reverse transcription PCR (AMV) from Roche was used. The first strand cDNA synthesis reaction was performed under the following conditions: 25°C for 10 min, 42°C for 60 min, 99°C for 5 min, and cooling to 4°C.

#### Real-time PCR

Real-time PCR amplification was deployed to quantify the gene expression of liver cell-specific factors applying the QuantiTect SYBR Green PCR Kit (Qiagen) in combination with human gene-specific QuantiTect Primer Assays (Qiagen). The details for the target genes are listed in Supplementary Table S3. Primers were tested for their human specificity before use. The expression of hepatocyte-specific factors was quantified using the comparative  $C_T$  method. Human Beta-actin (*ACTB*) was used as internal control. All reactions consisted of 12.5  $\mu$ L 2 $\times$  QuantiTect SYBR Green PCR Master Mix, 2.5  $\mu$ L 10 $\times$  QuantiTect Primer Assay, and 1  $\mu$ L cDNA as PCR template. The reactions were performed applying the StepOnePlus Real-time PCR System (Applied Biosystems, Foster City, CA). The cycling conditions were as follows: 95°C for 10 min followed by 45 cycles with 94°C for 15 s, 60°C for 30 s, and 72°C for 30 s. Melting curve analysis was performed routinely to verify the specificity of real-time PCR products. To further detect nonspecific amplifications real-time PCR products were transferred to a 2% agarose gel running in TRIS borate EDTA buffer at 80V/400 mA for 50 min.

#### Statistical analysis

Unpaired Student's *t*-test was used to compare the results of quantitative real-time PCR measurements.  $p < 0.05$  was accepted as significant whereas  $p < 0.01$  was considered as highly significant.

## Results

#### Isolation and maintenance of primary human hepatocytes in 3D cell culture

A mean cell viability of  $87.4\% \pm 12.3\%$  ( $n = 5$  isolations) was determined by Trypan blue test immediately after hepatocyte isolation (Table 1). Notably, isolation from a donor organ with 48 h of cold ischemia (Patient A) had an excellent outcome of 95% cell viability. Cell viabilities obtained from livers of metabolically disordered children were comparable with those achieved in hepatoblastoma or liver resection, respectively. All experimental steps involving liver cell isolation, *in vitro* spheroid formation, isolation, and transplantation in mice are summarized and displayed in Figure 1. In

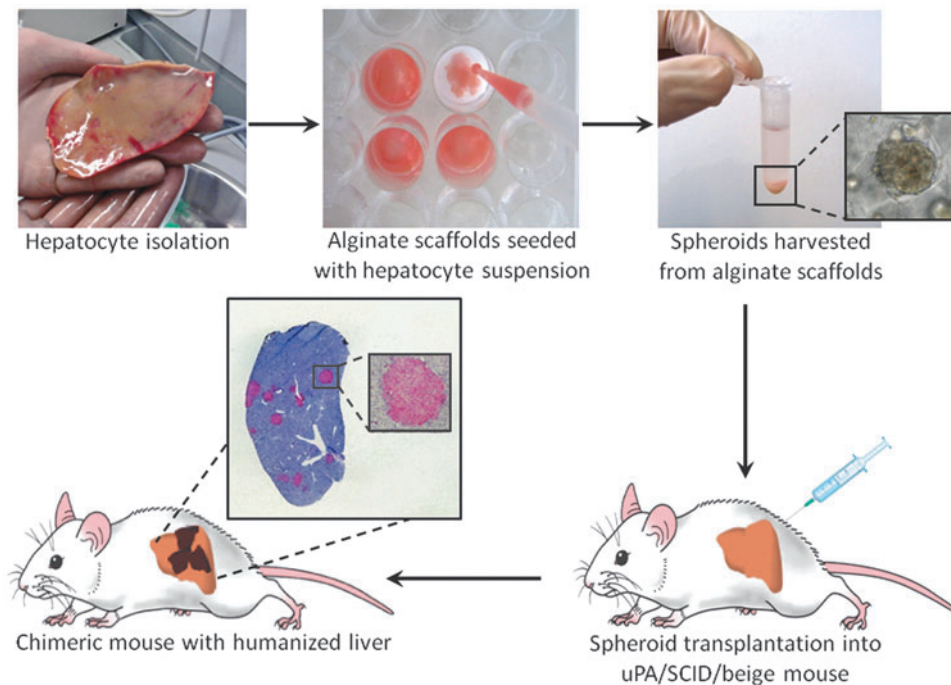


**FIG. 1.** Experimental design. Human hepatocytes isolated from donor livers were cultured on alginate scaffolds. After 7 days of preculture hepatocytes forming spheroids were harvested and transplanted into uPA/SCID/beige mice to investigate engraftment. A representative section of a humanized mouse liver 8 weeks after spheroid transplantation is shown. HumCK18 immunohistochemical staining (*red*) demonstrates human hepatocyte clusters in mouse livers, hematoxylin was used as background staining (*blue*). Color images available online at [www.liebertpub.com/tea](http://www.liebertpub.com/tea)

regard to the spheroid formation and as previously reported<sup>19</sup> hepatocyte aggregation within the pores of the scaffold was already observed after 24 h in 3D culture. From day 3 onward formation of spheroids was observed, which reached their maximum diameter (about 100–150  $\mu\text{m}$ ) at day 7.

#### *Human hepatocyte spheroids repopulate mouse livers after 7 days of preculture*

Primary human hepatocyte spheroids were transplanted into mice after 7 days.<sup>19</sup> Successful engraftment and *in vivo*

expansion of precultured human hepatocytes could be demonstrated in 11/33 animals that had been sacrificed 8 weeks after spheroid transplantation by visualization of humCK18. As shown in Figures 1 and 2, immunohistochemical staining of humCK18 revealed that human hepatocyte spheroids successfully reconstituted the diseased mouse liver parenchyma, since a uniform distribution of human clusters with a diameter between 200 and 3000  $\mu\text{m}$  was detected in all liver lobes. Human liver tissue was estimated to replace up to 30% of mouse liver tissue. No signs of tumor development, fibrosis, or cirrhosis were detected in

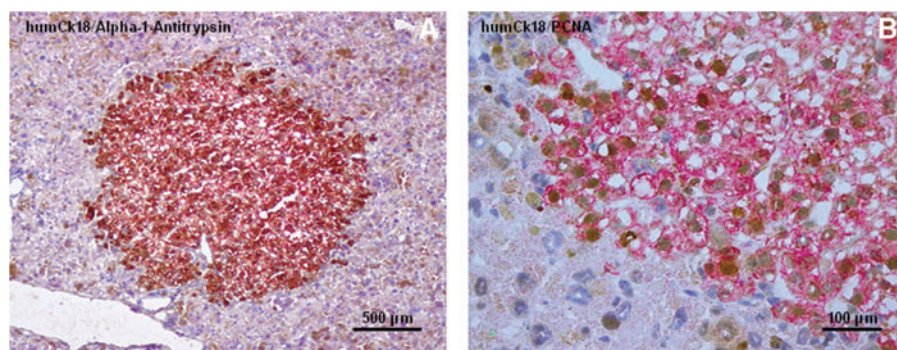


**FIG. 2.** Results of transmission light microscopy. (A) HumCK18 immunohistochemistry (*red*) for detection of human clusters was applied together with alpha-1-antitrypsin staining (A1A, *brown*). Hematoxylin was used as background staining (*blue*). Nearly all human hepatocytes displayed positive signal for A1A demonstrating the presence of highly functional hepatocytes in human clusters. (B) PCNA (*brown*) immunohistochemistry was used to demonstrate proliferation activity in combination with humCK18 (*red*) staining for detection of human clusters in mouse livers. Hematoxylin was applied as background staining (*blue*). Almost all human hepatocytes stained positive for PCNA indicating strong proliferative activity. A1A, alpha-1-antitrypsin; PCNA, proliferating cell nuclear antigen. Color images available online at [www.liebertpub.com/tea](http://www.liebertpub.com/tea)

TABLE 2. TRANSPLANTATION RESULTS

Patient	Transplanted mice	Mice positive for human hepatocytes	Human albumin in serum ( $\mu\text{g/mL}$ )	Human A1A in serum ( $\mu\text{g/mL}$ )
A	5	1	497	59.3
B	5	2	1312 1396	498 485
C	5	4	Not analyzed	Not analyzed
D	6	1	782	47.7
E	12	3	27.9 12.0 3.5	3.2 0.8 0.6
Total animals	33	11		

Successful human hepatocyte engraftment after spheroid transplantation could be demonstrated in 11/33 animals by visualization of the human cytoskeletal marker cytokeratin 18 (humCK18).

mouse livers. HumCK18 staining of spleens revealed no evidence of remaining human hepatocytes (data not shown).

*Precultured human hepatocytes retain their in vivo proliferation capacity and differentiation status in vivo*

To assess the presence of human hepatocyte-specific functions in mouse livers, we determined human serum albumin (HSA) concentration in mice 8 weeks after spheroid transplantation. Median HSA concentration was 576  $\mu\text{g/mL}$  but varied between 3.5 to 1396  $\mu\text{g/mL}$  in accordance with the repopulation rates achieved (Table 2). A1A production was demonstrated in human hepatocyte clusters as displayed in Figure 2A. We furthermore confirmed our histological

results using a human A1A ELISA test. Values ranged between 0.6 to 498  $\mu\text{g/mL}$  with a median human A1A concentration of 156  $\mu\text{g/mL}$  (Table 2).

Loss of proliferative capacity is commonly observed during hepatocyte cell culture. PCNA staining of humanized mouse livers revealed that despite 7 days in culture human hepatocytes retained their proliferation capacity *in vivo*. Interestingly, many hepatocytes in the border area of human clusters stained positive for PCNA indicating that proliferation activity was still ongoing 8 weeks after spheroid transplantation (Fig. 2B).

The human cytoskeletal marker CK18 was applied to distinguish between human and mouse hepatic tissue (Fig. 3A). Visualization of hepatocyte nuclear factor 4

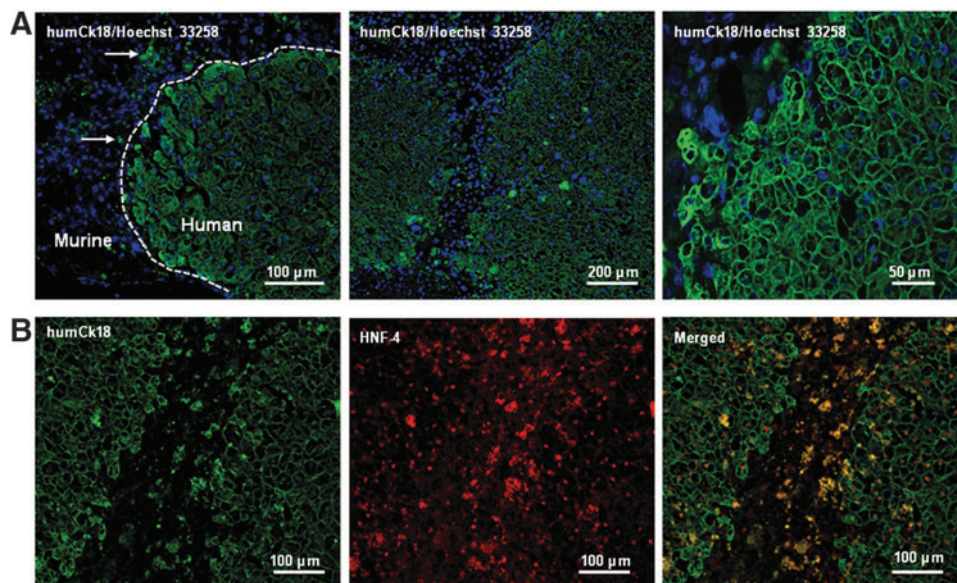


**FIG. 3.** Immunofluorescence staining of humanized mouse livers 8 weeks after spheroid transplantation. **(A)** HumCK18 (green) staining was performed to distinguish between human and mouse hepatic tissue. Hoechst 33258 (blue) was used as background staining. Successful human hepatocyte engraftment could be achieved in 11/33 transplanted animals. Human hepatocytes in mouse livers revealed excellent viability with well-organized physiological cytoskeletal network. In the left picture the border between human and mouse liver tissue is marked by a white line. Numerous macrophages (white arrows) were noticed as typically observed in young mice in this animal model. **(B)** Double staining of hepatocyte-specific transcription factor HNF-4 (red) and humCK18 (green). Positive nuclear staining of HNF-4 indicates highly preserved hepatocyte differentiation. HNF-4, hepatocyte nuclear factor 4. Color images available online at [www.liebertpub.com/tea](http://www.liebertpub.com/tea)

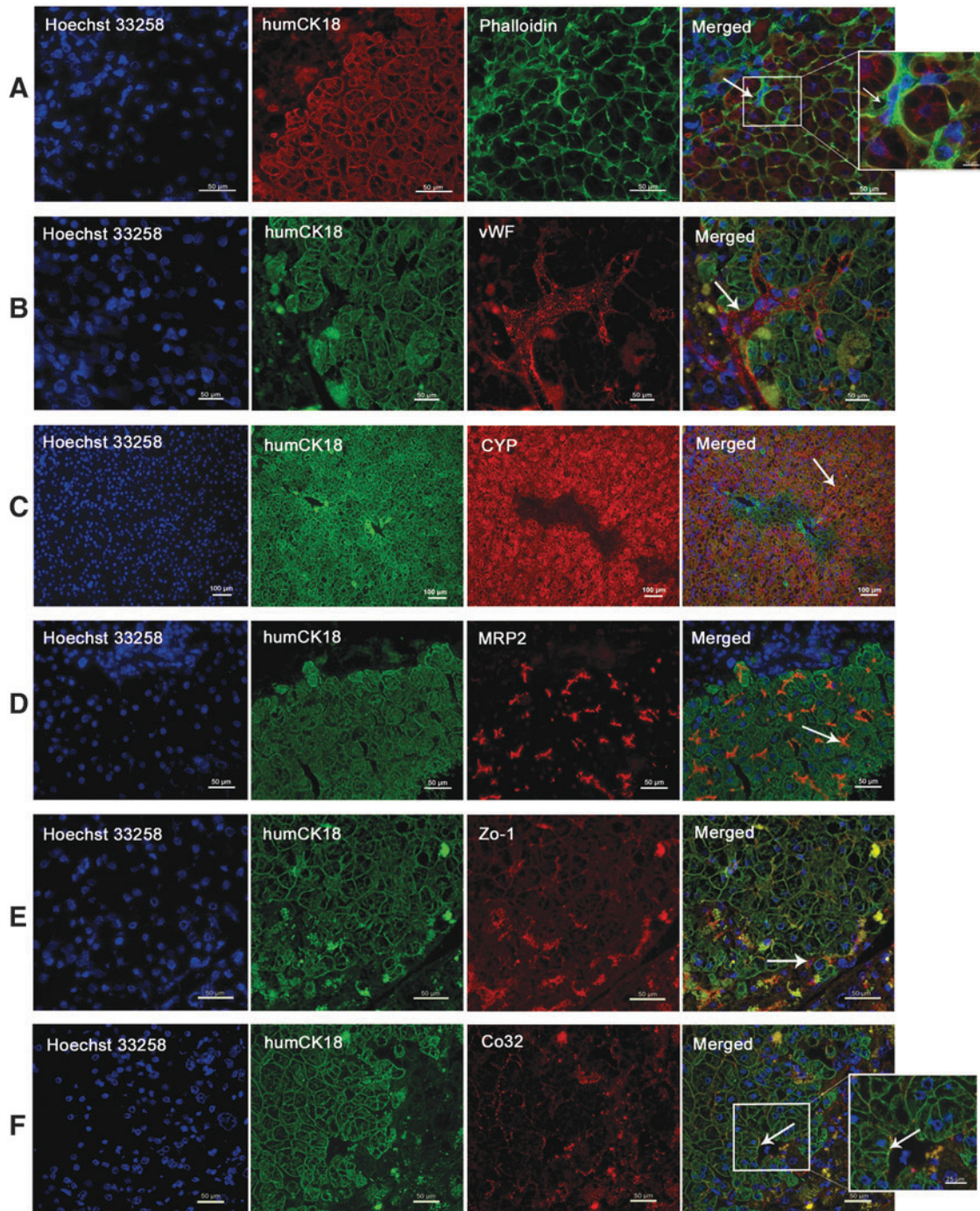


**FIG. 4.** Immunofluorescence staining of hepatocyte-specific factors in chimeric livers 8 weeks after spheroid transplantation. **(A)** For detection of actin filaments in bile canaliculi Alexa 488-labeled Phalloidin (*green*) was used. Re-formation of bile canaliculi between bordering hepatocytes was observed displaying the physiological micro-structure of the liver. A cross-sectioned bile canaliculus is marked by the *white arrow*. **(B)** Von Willebrand factor (vWF, *red*) labeling was performed to demonstrate vascularization of human tissue in mouse livers. Large vessels (*white arrow*) of mouse origin spread out into human clusters providing nutritional and oxygen supply along with waste removal. **(C)** Immunofluorescent staining of cytochrome P450 (CYP, *red*) revealed positive human hepatocytes in mouse livers indicating the ability to metabolize toxic substances (*white arrow*). **(D)** Multidrug resistance-associated protein 2 (MRP2) is predominantly found in the canalicular membrane of polarized hepatocytes. In our mouse model MRP2 (*red*) is visible as stripe between adjacent hepatocytes (*white arrow*) as also observed in physiological hepatic tissue. **(E)** Immunofluorescent staining of the tight junction protein zonula occludens protein 1 (ZO-1, *red*) was performed to demonstrate bipolar hepatocyte configuration in human clusters with apical and basolateral membrane. In our chimeric livers, tight junctions were detected not only between hepatocytes of one species but also between mouse and human hepatocytes (*white arrow*). **(F)** Immunofluorescent staining of the gap junction protein Connexin 32 (Co32, *red*) revealed positive signaling not only between human hepatocytes, but also between hepatocytes of the two different species (*white arrow*) indicating highly differentiated hepatocyte interaction, enabling cell-to-cell communication. HumCK18 (*green/red*) labeling was applied in all of our immunofluorescent stainings to distinguish between human and mouse hepatic tissue. Hoechst 33258 (*blue*) was used as counterstaining for viable cell nuclei. Color images available online at [www.liebertpub.com/tea](http://www.liebertpub.com/tea)

(HNF-4) alpha was performed to observe the state of cell differentiation. Nearly all human hepatocytes displayed positive nuclear transcription factor HNF-4, indicating that hepatocyte differentiation is highly retained in transplanted cells (Fig. 3B).

Phalloidin staining was established for detection of actin filaments that are localized in bile canaliculi. Bile canaliculi network embracing mouse and human hepatocytes was detected in chimeric livers displaying liver tissue-specific microstructure (Fig. 4A).

Von Willebrand factor (vWF) activity demonstrated vascularization of human clusters in mouse livers. Small capillaries, and large blood vessels, were detected both within human clusters and spread out from mouse liver areas into human clusters (Fig. 4B). As a result of species-specific CD31 staining it could be clarified that the vessels were of mouse origin (pictures not shown).

As displayed in Figure 4C, positive CYP2E1 staining of human hepatocytes in mouse livers indicated that pre-cultured hepatocytes maintained their capability to metabolize potentially toxic compounds.

Multidrug resistance-associated protein 2 (MRP2) is predominantly found in the canalicular membrane of polarized hepatocytes and mediates biliary excretion of endogenous or exogenous substances.<sup>27</sup> Analysis of MRP2 localization in human clusters within the chimeric livers revealed not only positive staining but also a distribution resembling normal human liver tissues (Fig. 4D).

Zonula occludens protein 1 (ZO-1) is a marker for tight junctions that indicates bile canaliculi formation and bipolar hepatocyte configuration in liver tissue.<sup>28,29</sup> In our chimeric livers tight junctions were detected not only between hepatocytes of one species but also between mouse and human

hepatocytes as displayed in Figure 4E. Moreover, positive staining of the gap junction protein connexin 32 (Cx32) indicated intercellular communication.<sup>30</sup> Positive staining for this marker was also observed both between human hepatocytes and between hepatocytes of the two different species (Fig. 4F).

Altogether, no encapsulation and no strict border between the hepatocytes of the different species were observed, indicating excellent integration of human hepatocyte spheroids in mouse liver parenchyma. Moreover, humCK18 visualization and Hoechst 33258 nuclear counterstaining revealed that human hepatocytes in mouse livers were well organized with physiological cytoskeletal network (Figs. 3 and 4). Our results with ARG1/GLUL staining show that there was no structural heterogeneity relative to hepatocyte location in human clusters. Nearly all human hepatocytes in mouse livers stained slightly positive for both markers (Supplementary Figs. S2 and S3).

To investigate the gene expression profile of human hepatocytes in chimeric mouse livers, quantitative real-time PCR measurements were performed. Figure 5 summarizes results of liver-specific human genes obtained in mice in comparison with native human tissue, freshly isolated human hepatocytes, and cultured hepatocytes. Nearly constant *Alb* mRNA expression was observed in native tissue and freshly isolated cells, respectively, whereas *Alb* gene expression in cultured cells decreased as expected.

*CYP1A2* expression levels decreased at the beginning of the cell culture and increased thereafter as a result of *CYP* induction. *CYP3A4* induction was already low in the basic tissue and below detection limit in the cultured cells. Copy numbers of transferrin and phase II enzyme glutathione S-transferase (*GSTA1*) decreased after cell isolation but

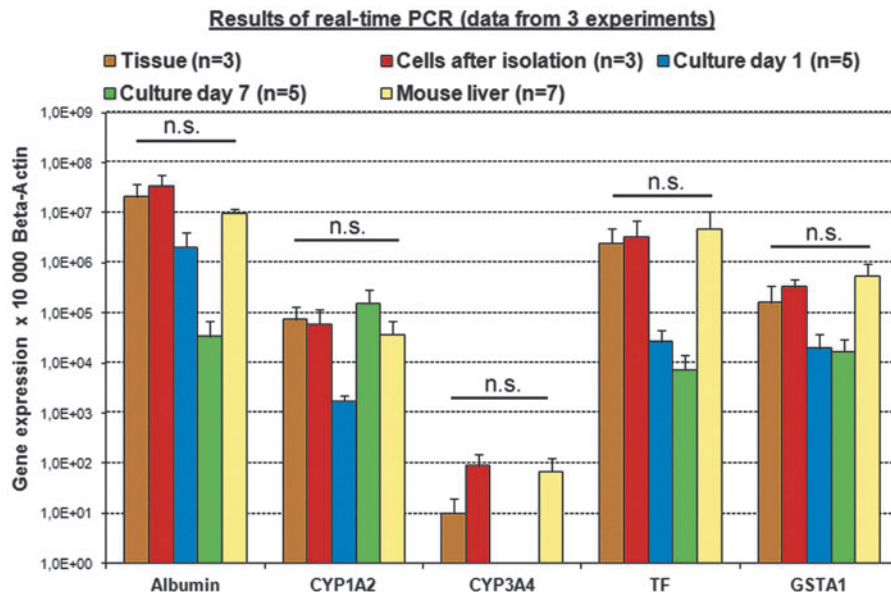


**FIG. 5.** Results of real-time PCR. Gene expression pattern of human hepatocytes in native tissue before cell isolation compared to freshly isolated cells (three experiments), cells on alginate scaffolds after 1 and 7 days of culture ( $n = 5/t$ , three experiments) and *in vivo* expression of human hepatocytes in mouse livers ( $n = 7$ , three experiments). ACTB was used as internal control. The values are expressed as mean  $\pm$  SD. *In vivo* expression levels of all analyzed human genes in mice were nearly identical compared to expression levels in native human tissue before cell isolation. Statistical analysis revealed no significant differences between these two groups. CYP, cytochrome P450; GSTA1, glutathione S-transferase; n.s., not significant; TF, transferrin. Color images available online at [www.liebertpub.com/tea](http://www.liebertpub.com/tea)

remained constant during the entire culture period. Remarkably, *in vivo* expression levels of all human genes analyzed appeared almost identical in chimeric mouse livers compared to expression levels determined in native human liver tissue before cell isolation. Statistical analysis revealed no significant differences between these two groups. Melting curve analysis resulted in a single-specific peak for each amplified product demonstrating the specificity of real-time PCR (Supplementary Fig. S1A). To further validate real-time PCR products were separated on 2% agarose gels. Only single specific bands were observed for each PCR indicating the absence of nonspecific amplification (Supplementary Fig. S1B).

#### Efficient engraftment of RGB-marked cells

Simultaneous hepatocyte transduction with three LeGO vectors encoding red, green, or blue fluorescent proteins was performed in experiment C after 6 days of preculture. Fluorescent imaging obtained right before spheroid transplantation into mice confirmed effective multi-color labeling of human hepatocytes. The three basic colors, but also numerous hues resulting from their mixtures can be distinguished (Fig. 6A). Fluorescent microscopic imaging of explanted livers demonstrated stable RGB marking of human hepatocyte clusters that originated upon multiple rounds of cell divisions (Figs. 6B–D). As previously reported,<sup>24</sup> we predominantly

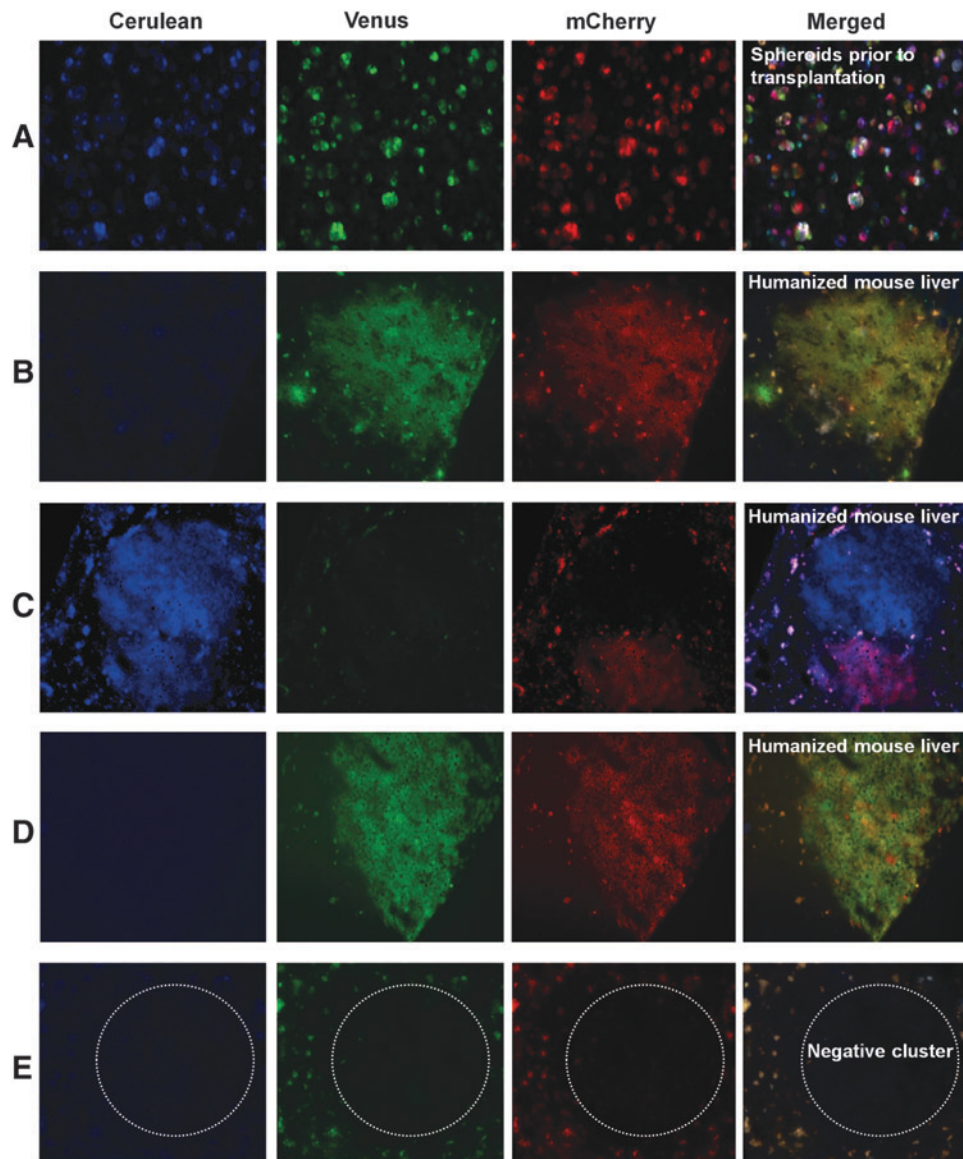


**FIG. 6.** Results of *in vitro* lentiviral transduction. (A) Fluorescent imaging *right* before spheroid transplantation revealed high-rate lentiviral transduction of primary hepatocytes with the three LeGO vectors encoding mCherry (*red*), Venus (*green*) and Cerulean (*blue*). Simultaneous presence of these three basic colors in individual cells resulted in efficient RGB marking (*merged image*). (B–D) Fluorescent microscopic imaging of explanted livers showed stable *in vivo* *red*, *green*, and *blue* labeling in human clusters upon multiple rounds of cell divisions. (E) Just a few human clusters remained negative for RGB marking. LeGO, Lentiviral Gene Ontology; RGB, red-green-blue. Color images available online at [www.liebertpub.com/tea](http://www.liebertpub.com/tea)

found clusters of human hepatocytes displaying the same RGB marking pattern, revealing monoclonal expansion of individual human hepatocytes that successfully engrafted the mouse livers at a given spot. Since the overall transduction rates were below 100% as expected, a few human clusters remained negative for RGB marking (Fig. 6E).

## Discussion

Liver transplantation is the preferred therapy for patients with end-stage liver diseases or liver-based inherited metabolic disorders. Nevertheless, due to organ shortage alternative treatments such as hepatocyte transplantation have been developed and clinically applied in selected cases.<sup>6-9</sup> Unfortunately, the success of this treatment has been limited by low cell engraftment rates and the restricted sources of human hepatocytes. We previously showed that hepatocytes obtained from children with inherited metabolic disorders form highly differentiated human hepatocyte spheroids that preserved metabolic activities even after 7 days of culture.<sup>19</sup> Herewith, we used the well-established uPA mouse model of liver regeneration to assess the regenerative potential of such precultured spheroids *in vivo*.

The levels of human liver chimerism commonly achieved in uPA mice are known to vary strongly among transplanted animals and depend both on the different rates of initially engrafted hepatocytes and on the capacities of these cells to expand *in vivo*. Although we observed a large but not unusual variety in human HSA and A1A concentrations and repopulation rates among transplanted mice, large human hepatocyte clusters were determined in mice that had been successfully engrafted with spheroid-derived primary human hepatocytes.

It is known that *in vitro* loss of proliferative capacity is one of the most restricting problems during hepatocyte culture. As determined by the presence of large human hepatocyte clusters and PCNA staining in transplanted mice, we demonstrated that the precultured hepatocytes could regain their proliferation capacity *in vivo*.

Extensive histological examinations were performed to confirm physiological morphology of human hepatocyte clusters in mouse livers. HNF-4 is one of the major liver-specific transcription factors and participates in the regulation of several genes involved in liver-derived metabolic pathways.<sup>31</sup> In our model almost all human hepatocytes revealed positive staining 8 weeks after transplantation, indicating the maintenance of highly differentiated human hepatocytes forming human liver tissue within the mouse livers.

ZO-1 is known to be located in the intercellular tight junctions indicating maintenance of cell polarity. Positive staining of ZO-1 together with actin filament labeling by phalloidin revealed re-formation of bile canaliculi and bipolar configuration between adjacent human hepatocytes in mouse livers. Notably, tight junctions were not only detected between human hepatocytes but also between mouse and human hepatocytes. These findings are highly relevant, since isolated hepatocytes lose their polarized structure after dissociation from liver tissue.<sup>28</sup>

To prove *in vivo* angiogenesis of human clusters vWF activity was analyzed. We observed both small capillaries and large vessels within human hepatocyte clusters providing nutritional and oxygen supply and waste removal.

One of the most important hepatocyte functions is their ability to metabolize drugs and toxic substances. We stained CYP2E1 as an important member of the *CYP* gene family enabling, for instance, ethanol and paracetamol detoxification in humans.<sup>32</sup> The presence of positive human hepatocytes 8 weeks after spheroid transplantation suggests maintenance of detoxification capacity.

Moreover, the localization of MRP2 in the apical membrane of polarized epithelia favors a particular role of this isoform in detoxification pathway.<sup>33</sup> The presence of MRP2 with physiological distribution in our humanized livers indicates that efficient terminal excretion of conjugated drug metabolism products via bilious flow is possible.

In physiological liver tissue, there is a strong functional interaction between neighboring cells. It was therefore not surprising to identify Co32-positive junctional complexes between adjacent hepatocytes in human clusters maintaining cell-to-cell communication. However, gap junction re-formation between hepatocytes of the different species was surprising, since it has been described that for intercellular channel formation each cell should provide one hemi-channel.<sup>34</sup>

Our histological investigations identified highly differentiated human liver areas within the mouse liver parenchyma, whereas gene expression analysis confirmed that human cells expressed typical hepatocyte-specific functions. Of note, a decreased gene expression was observed during the 7-day culture period, probably as a consequence of the isolation procedure and culture conditions. Nevertheless, the *in vivo* expression levels of all analyzed human genes increased to the basic levels determined in the native liver before cell isolation, thus demonstrating the regain of the hepatocyte-specific gene expression profile *in vivo*, upon transplantation in mice.

Several methods for gene transfer into hepatocytes have been developed, including *ex vivo* and *in vivo* approaches using viral or nonviral vector systems leading to transient, nearly stable or stable gene expression. The use of lentiviral vectors has several advantages in our setup and may serve as a proof-of-concept for the permanent genetic modification of hepatocytes *ex vivo*. Within the scaffolds, hepatocytes can be kept in culture for several days, allowing a quality check of the gene transfer before transplantation of the cells. The *ex vivo* gene transfer into purified cells allows a specific targeting of hepatocytes and in addition avoids any dissemination or transduction of any unwanted cell types like professional antigen-presenting cells, thereby helping to evade an immune response as compared to the *in vivo* application of the vectors. Since after transplantation the cells are dividing several times, their stable modification by the applied lentiviral vectors is a prerequisite for a sustained transgene expression in all daughter cells after engraftment and expansion. Recently, efficient tools for genome engineering, particularly as CRISPR/Cas9, have become available providing an alternative possibility for stable genome modifications.<sup>35</sup> However, efficient delivery of the required designer nucleases remains a challenge. Nonintegrating lentiviral vectors have been suggested as an efficient delivery vehicle for CRISPR/Cas9.<sup>36</sup>

Altogether, this technique could be a promising option for patients with inherited metabolic disorders because their disease is mostly based on a single enzyme deficiency and their liver otherwise functions normally. The finding that

RGB marked human hepatocytes engrafted and significantly expanded *in vivo* to form human clusters repopulating the diseased mouse liver thus represents an important step toward potential future therapeutic applications.

Recently, there has been a focus on deriving human hepatocytes from other sources than human donor livers, in particular human embryonic stem cells (ESCs) and human induced pluripotent stem cells (iPSCs) suggesting an application in the field of cell-based therapies and drug screening.<sup>37–47</sup> One of the advantages is that stem cell-derived cells may provide an unlimited supply of hepatocytes. Although there have been improvements increasing differentiation efficiency of stem cells to functional hepatocytes, current strategies still yield relatively heterogeneous populations.<sup>40</sup> However, there are efforts to develop a process for the manufacturing of iPSC master cell banks under current good manufacturing practice and such banks became already available.<sup>48</sup> One of the most important challenges of these new techniques is that tumor formation has been a concern associated with ESC- or iPSC-based cellular therapy.<sup>37</sup> A recently published *in vivo* study applying a mouse model of liver injury revealed that after transplantation of ESC-derived hepatocyte-like cells all murine recipients developed large splenic and liver tumors that contained endodermal and mesodermal cell types. Although such studies demonstrate that ESC-derived cells have the potential to play an important role in cell-based therapies, current methodologies and transplantation strategies require substantial refinement before they can be deployed safely.<sup>42</sup> In contrast, no signs of tumor development were detected in our applied mouse model indicating that the use of primary human hepatocytes after preculture is with lower risk for the prospective recipient. But nevertheless, those stem cell-derived models hold great potential to develop a detailed understanding of human liver disease and metabolism including drug toxicity.<sup>44</sup>

In summary, our results demonstrate successful liver repopulation with precultured human hepatocytes indicating that such procedures may offer new opportunities to bridge the availability of highly differentiated hepatocytes from a donor liver in anticipation of an appropriate recipient. Also, the possibility to obtain human hepatocytes directly from a patient and to transplant them back after therapeutic modification is very encouraging. On the other hand, in the applied mouse model, hepatic expression of the uPA transgene causes liver damage resulting in destruction of mouse endogenous hepatocytes and enhanced proliferation of transplanted hepatocytes. To this regard, the model strongly resembles toxic liver failure in humans. However, in livers of patients with inherited metabolic disorders preparative regimen such as partial hepatectomy might be necessary before transplantation to enhance engraftment of the transplanted spheroids.<sup>49</sup>

In conclusion, this is the first report demonstrating that human hepatocyte spheroids obtained after 7 days preculture and *in vitro* lentiviral gene transfer are able to repopulate a recipient liver. In future, transplantation of these spheroids into a liver-diseased recipient could present a real alternative to liver transplantation.

#### Acknowledgments

The authors would like to thank R. Goswami and A. Schmidt for their technical assistance and A. Groth and R.

Reusch for excellent care of the mouse colony in Hamburg. The study was supported by a grant from the BONFOR-Forschungskommission (O-112.0049), University of Bonn, Germany and the SFB841 (C7 to BF).

#### Disclosure Statement

No competing financial interests exist.

#### References

- Pietrosi, G., Vizzini, G.B., Gruttadauria, S., and Gridelli, B. Clinical applications of hepatocyte transplantation. *World J Gastroenterol* **15**, 2074, 2009.
- Turner, R., Gerber, D., and Reid, L. The future of cell transplant therapies: a need for tissue grafting. *Transplantation* **90**, 807, 2010.
- Horslen, S.P., and Fox, I.J. Hepatocyte transplantation. *Transplantation* **77**, 1481, 2004.
- Vogel, K., Kennedy, A., Whitehouse, L., and Gibson, K.M. Therapeutic hepatocyte transplant for inherited metabolic disorders: functional considerations, recent outcomes and future prospects. *J Inherit Metab Dis* **37**, 165, 2014.
- Fisher, R.A., Bu, D., Thompson, M., Tisnado, J., Prasad, U., Sterling, R., Posner, M., and Strom, S. Defining hepatocellular chimerism in a liver failure patient bridged with hepatocyte infusion. *Transplantation* **69**, 303, 2000.
- Schneider, A., Attaran, M., Meier, P.N., Strassburg, C., Manns, M.P., Ott, M., Barthold, M., Arseniev, L., Becker, T., and Panning, B. Hepatocyte transplantation in an acute liver failure due to mushroom poisoning. *Transplantation* **82**, 1115, 2006.
- Fitzpatrick, E., Mitry, R.R., and Dhawan, A. Human hepatocyte transplantation: state of the art. *J Intern Med* **266**, 339, 2009.
- Meyburg, J., Schmidt, J., and Hoffmann, G.F. Liver cell transplantation in children. *Clin Transplant* **23(Suppl 21)**, 75, 2009.
- Meyburg, J., and Hoffmann, G.F. Liver cell transplantation for the treatment of inborn errors of metabolism. *J Inherit Metab Dis* **31**, 164, 2008.
- Soltys, K.A., Soto-Gutiérrez, A., Nagaya, M., Baskin, K.M., Deutsch, M., Ito, R., Schneider, B.L., Squires, R., Vockley, J., Guha, C., Roy-Chowdhury, J., Strom, S.C., Platt, J.L., and Fox, I.J. Barriers to the successful treatment of liver disease by hepatocyte transplantation. *J Hepatol* **53**, 769, 2010.
- Hewitt, N.J., Lechon, M.J., Houston, J.B., Hallifax, D., Brown, H.S., Maurel, P., Kenna, J.G., Gustavsson, L., Lohmann, C., Skonberg, C., Guillouzo, A., Tuschl, G., Li, A.P., LeCluyse, E., Groothuis, G.M., and Hengstler, J.G. Primary hepatocytes: current understanding of the regulation of metabolic enzymes and transporter proteins, and pharmaceutical practice for the use of hepatocytes in metabolism, enzyme induction, transporter, clearance, and hepatotoxicity studies. *Drug Metab Rev* **39**, 159, 2007.
- Dandri, M., Burda, M.R., Gocht, A., Torok, E., Pollok, J.M., Rogler, C.E., Will, H., and Petersen, J. Woodchuck hepatocytes remain permissive for hepadnavirus infection and mouse liver repopulation after cryopreservation. *Hepatology* **34(4 Pt 1)**, 824, 2001.
- Torok, E., Lutgehetmann, M., Bierwolf, J., Melbeck, S., Dullmann, J., Nashan, B., Ma, P.X., and Pollok, J.M. Primary human hepatocytes on biodegradable poly(l-lactic

- acid) matrices: a promising model for improving transplantation efficiency with tissue engineering. *Liver Transpl* **17**, 104, 2011.
14. Torok, E., Pollok, J.M., Ma, P.X., Kaufmann, P.M., Dandri, M., Petersen, J., Burda, M.R., Kluth, D., Perner, F., and Rogiers, X. Optimization of hepatocyte spheroid formation for hepatic tissue engineering on three-dimensional biodegradable polymer within a flow bioreactor before implantation. *Cells Tissues Organs* **169**, 34, 2001.
  15. Torok, E., Pollok, J.M., Ma, P.X., Kaufmann, P.M., Dandri, M., Petersen, J., Burda, M.R., Kluth, D., Perner, F., and Rogiers, X. Pre-implantation optimization of culture conditions for hepatocytes in a flow bioreactor for hepatic tissue engineering on 3-dimensional biodegradable polymers. *Zentralblatt für Kinderchirurgie* **11**, 188, 2002.
  16. Torok, E., Pollok, J.M., Ma, P.X., Vogel, C., Dandri, M., Petersen, J., Burda, M.R., Kaufman, P.M., Kluth, D., and Rogiers, X. Hepatic tissue engineering on 3-dimensional biodegradable polymers within a pulsatile flow bioreactor. *Dig Surg* **18**, 196, 2001.
  17. Torok, E., Vogel, C., Lutgehetmann, M., Ma, P.X., Dandri, M., Petersen, J., Burda, M.R., Siebert, K., Dullmann, J., Rogiers, X., and Pollok, J.M. Morphological and functional analysis of rat hepatocyte spheroids generated on poly(L-lactic acid) polymer in a pulsatile flow bioreactor. *Tissue Eng* **12**, 1881, 2006.
  18. Bierwolf, J., Lutgehetmann, M., Feng, K., Erbes, J., Deichmann, S., Toronyi, E., Stieglitz, C., Nashan, B., Ma, P.X., and Pollok, J.M. Primary rat hepatocyte culture on 3D nanofibrous polymer scaffolds for toxicology and pharmaceutical research. *Biotechnol Bioeng* **108**, 141, 2011.
  19. Bierwolf, J., Lutgehetmann, M., Deichmann, S., Erbes, J., Volz, T., Dandri, M., Cohen, S., Nashan, B., and Pollok, J.M. Primary human hepatocytes from metabolic-disordered children recreate highly differentiated liver-tissue-like spheroids on alginate scaffolds. *Tissue Eng Part A* **18**, 1443, 2012.
  20. Lee, K.Y., and Mooney, D.J. Alginate: properties and biomedical applications. *Prog Polym Sci* **37**, 106, 2012.
  21. Sandgren, E.P., Palmiter, R.D., Heckel, J.L., Daugherty, C.C., Brinster, R.L., and Degen, J.L. Complete hepatic regeneration after somatic deletion of an albumin-plasminogen activator transgene. *Cell* **66**, 245, 1991.
  22. Rhim, J.A., Sandgren, E.P., Degen, J.L., Palmiter, R.D., and Brinster, R.L. Replacement of diseased mouse liver by hepatic cell transplantation. *Science* **263**, 1149, 1994.
  23. Petersen, J., Burda, M.R., Dandri, M., and Rogler, C.E. Transplantation of human hepatocytes in immunodeficient UPA mice: a model for the study of hepatitis B virus. *Methods Mol Med* **96**, 253, 2004.
  24. Weber, K., Thomaschewski, M., Warlich, M., Volz, T., Cornils, K., Niebuhr, B., Tager, M., Lutgehetmann, M., Pollok, J.M., Stocking, C., Dandri, M., Benten, D., and Fehse, B. RGB marking facilitates multicolor clonal cell tracking. *Nat Med* **17**, 504, 2011.
  25. Weber, K., Thomaschewski, M., Benten, D., and Fehse, B. RGB marking with lentiviral vectors for multicolor clonal cell tracking. *Nat Protoc* **7**, 839, 2012.
  26. Lutgehetmann, M., Mancke, L.V., Volz, T., Helbig, M., Allweiss, L., Bornscheuer, T., Pollok, J.M., Lohse, A.W., Petersen, J., Urban, S., and Dandri, M. Humanized chimeric uPA mouse model for the study of hepatitis B and D virus interactions and preclinical drug evaluation. *Hepatology* **55**, 685, 2012.
  27. Hu, Y., Sampson, K.E., Heyde, B.R., Mandrell, K.M., Li, N., Zutshi, A., and Lai, Y. Saturation of multidrug-resistant protein 2 (mrp2/abcc2)-mediated hepatobiliary secretion: nonlinear pharmacokinetics of a heterocyclic compound in rats after intravenous bolus administration. *Drug Metab Dispos* **37**, 841, 2009.
  28. Abu-Absi, S.F., Friend, J.R., Hansen, L.K., and Hu, W.S. Structural polarity and functional bile canaliculi in rat hepatocyte spheroids. *Exp Cell Res* **274**, 56, 2002.
  29. Fanning, A.S., and Anderson, J.M. Zonula occludens-1 and -2 are cytosolic scaffolds that regulate the assembly of cellular junctions. *Ann N Y Acad Sci* **1165**, 113, 2009.
  30. Piechocki, M.P., Toti, R.M., Fernstrom, M.J., Burk, R.D., and Ruch, R.J. Liver cell-specific transcriptional regulation of connexin32. *Biochim Biophys Acta* **1491**, 107, 2000.
  31. Schrem, H., Klempnauer, J., and Borlak, J. Liver-enriched transcription factors in liver function and development. Part I: the hepatocyte nuclear factor network and liver-specific gene expression. *Pharmacol Rev* **54**, 129, 2002.
  32. Martignoni, M., Groothuis, G.M., and de Kanter, R. Species differences between mouse, rat, dog, monkey and human CYP-mediated drug metabolism, inhibition and induction. *Expert Opin Drug Metab Toxicol* **2**, 875, 2006.
  33. Konig, J., Nies, A.T., Cui, Y., Leier, I., and Keppler, D. Conjugate export pumps of the multidrug resistance protein (MRP) family: localization, substrate specificity, and MRP2-mediated drug resistance. *Biochim Biophys Acta* **1461**, 377, 1999.
  34. Sáez, J.C., Retamal, M.A., Basilio, D., Bukauskas, F.F., and Bennett, M.V.L. Connexin-based gap junction hemichannels: Gating mechanisms. *Biochim Biophys Acta* **1711**, 215, 2005.
  35. Aravalli, R.N., Belcher, J.D., and Steer, C.J. Liver-targeted gene therapy: approaches and challenges. *Liver Transpl* **21**, 718, 2015.
  36. Shalem, O., Sanjana, N.E., Hartenian, E., Shi, X., Scott, D.A., Mikkelsen, T.S., Heckl, D., Ebert, B.L., Root, D.E., Doench, J.G., and Zhang, F. Genome-scale CRISPR-Cas9 knockout screening in human cells. *Science* **343**, 84, 2014.
  37. Liu, H., Kim, Y., Sharkis, S., Marchionni, L., and Jang, Y.Y. In vivo liver regeneration potential of human induced pluripotent stem cells from diverse origins. *Sci Translational Med* **3**, 82, 2011.
  38. Duan, Y., Catana, A., Meng, Y., Yamamoto, N., He, S., Gupta, S., Gambhir, S.S., and Zern, M.A. Differentiation and enrichment of hepatocyte-like cells from human embryonic stem cells in vitro and in vivo. *Stem Cells* **25**, 3058, 2007.
  39. Hay, D.C., Zhao, D., Ross, A., Mandalam, R., Lebkowski, J., and Cui, W. Direct differentiation of human embryonic stem cells to hepatocyte-like cells exhibiting functional activities. *Cloning Stem Cells* **9**, 51, 2007.
  40. Hay, D.C., Fletcher, J., Payne, C., Terrace, J.D., Gallagher, R.C., Snoeys, J., Black, J.R., Wojtacha, D., Samuel, K., Hannoun, Z., Pryde, A., Filippi, C., Currie, I.S., Forbes, S.J., Ross, J.A., Newsome, P.N., and Iredale, J.P. Highly efficient differentiation of hESCs to functional hepatic endoderm requires ActivinA and Wnt3a signaling. *Proc Natl Acad Sci U S A* **105**, 12301, 2008.
  41. Cai, J., Zhao, Y., Liu, Y., Ye, F., Song, Z., Qin, H., Meng, S., Chen, Y., Zhou, R., Song, X., Guo, Y., Ding, M., and Deng, H. Directed differentiation of human embryonic stem cells into functional hepatic cells. *Hepatology* **45**, 1229, 2007.
  42. Payne, C.M., Samuel, K., Pryde, A., King, J., Brownstein, D., Schrader, J., Medine, C.N., Forbes, S.J., Iredale, J.P.,

- Newsome, P.N., and Hay, D.C. Persistence of functional hepatocyte-like cells in immune-compromised mice. *Liver Int* **31**, 254, 2011.
43. Si-Tayeb, K., Noto, F.K., Nagaoka, M., Li, J., Battle, M.A., Duris, C., North, P.E., Dalton, S., and Duncan, S.A. Highly efficient generation of human hepatocyte-like cells from induced pluripotent stem cells. *Hepatology* **51**, 297, 2010.
44. Sullivan, G.J., Hay, D.C., Park, I.H., Fletcher, J., Hannoun, Z., Payne, C.M., Dalgetty, D., Black, J.R., Ross, J.A., Samuel, K., Wang, G., Daley, G.Q., Lee, J.H., Church, G.M., Forbes, S.J., Iredale, J.P., and Wilmot, I. Generation of functional human hepatic endoderm from human induced pluripotent stem cells. *Hepatology* **51**, 329, 2010.
45. Szkolnicka, D., Farnworth, S.L., Lucendo-Villarin, B., and Hay, D.C. Deriving functional hepatocytes from pluripotent stem cells. *Curr Protoc Stem Cell Biol* **30**, 1G.5.1-12, 2014.
46. Holmgren, G., Sjogren, A.K., Barragan, I., Sabirsh, A., Sartipy, P., Synnergren, J., Bjorquist, P., Ingelman-Sundberg, M., Andersson, T.B., and Edsbacke, J. Long-term chronic toxicity testing using human pluripotent stem cell-derived hepatocytes. *Drug Metab Dispos* **42**, 140, 2014.
47. Villarin, B.L., Cameron, K., Szkolnicka, D., Rashidi, H., Bates, N., Kimber, S.J., Flint, O., Forbes, S.J., Iredale, J.P., Bradley, M., and Hay, D.C. Polymer Supported Directed Differentiation Reveals a Unique Gene Signature Predicting Stable Hepatocyte Performance. *Adv Healthcare Mater* **4**, 1820, 2015.
48. Baghbaderani, B.A., Tian, X., Neo, B.H., Burkall, A., Dimmezzo, T., Sierra, G., Zeng, X., Warren, K., Kovarcik, D.P., Fellner, T., and Rao, M.S. cGMP-Manufactured Human Induced Pluripotent Stem Cells Are Available for Pre-clinical and Clinical Applications. *Stem Cell Rep* **5**, 647, 2015.
49. Yamanouchi, K., Zhou, H., Roy-Chowdhury, N., Macaluso, F., Liu, L., Yamamoto, T., Yannam, G.R., Enke, C., Solberg, T.D., Adelson, A.B., Platt, J.L., Fox, I.J., Roy-Chowdhury, J., and Guha, C. Hepatic irradiation augments engraftment of donor cells following hepatocyte transplantation. *Hepatology* **49**, 258, 2009.

Address correspondence to:  
*Joerg-Matthias Pollok, MD, PhD*  
*Department for General, Visceral, Thoracic,*  
*and Vascular Surgery*  
*University Medical Center Bonn*  
*Sigmund-Freud-Street 25*  
*Bonn 53105*  
*Germany*

*E-mail: joerg.pollok@ukb.uni-bonn.de*

*Received: September 9, 2015*

*Accepted: April 11, 2016*

*Online Publication Date: May 4, 2016*